Editors' Suggestion

Many-body vertex effects: Time-dependent interaction kernel with correlated multiexcitons in the Bethe-Salpeter equation

Brian Cunningham
NI-HPC, Queen's University Belfast, Belfast BT7 1NN, United Kingdom

(Received 4 March 2025; revised 29 August 2025; accepted 3 September 2025; published 29 September 2025)

Building on a beyond-*GW* many-body perturbative framework that incorporates higher-order vertex effects in the self-energy—giving rise to T-matrix and second-order exchange contributions—this approach is extended to now include the vertex derived in that work to the kernel in the Bethe-Salpeter equation (BSE) for the reducible polarization function. This results in a frequency-dependent interaction kernel that naturally captures random phase approximation effects, dynamical excitonic interactions, and the correlated propagation of multiple correlated electron-hole pairs that model multiexcitonic (including bi- and triexcitonic) effects, relevant for nonlinear optics and high-harmonic generation. These processes emerge as a result of including the functional derivatives of the screening and vertex with respect to the Green's function in the vertex, enabling a fully *ab initio*, time-dependent treatment of correlation effects. By focusing on the reducible rather than irreducible polarization function, this approach provides a computationally viable framework for capturing complex many-body interactions for calculating the self-energy, optical spectra, and electron energy loss spectroscopy. The resulting interaction kernel is relatively straightforward, clearly delineates the physical processes that are included and omitted, and has the same dimensionality as the conventional BSE kernel used in standard many-body perturbation theory implementations but is now itself frequency dependent. The method is expected to facilitate the integration of advanced many-body effects into state-of-the-art software packages, offering a universal and highly accurate framework for the description of subatomic correlations. Such advancements are crucial for the development of semiconductor, optoelectronic, superconducting, and antimatter technologies and ensuring that theoretical modeling evolves alongside exascale and accelerated computing.

DOI: 10.1103/6vsh-ck4q

I. INTRODUCTION

Advancing our understanding of subatomic particle interactions, such as electron-electron, electron-nucleus, and electron-positron interactions, is essential for increasing our understanding of the universe and driving progress in technology, medicine, and computation. The Kohn-Sham formulation of density functional theory (DFT) [1,2] is the most widely used method for studying electronic interactions due to its balance of accuracy and efficiency. DFT continues to evolve, being applied to real-world problems; however, despite the success of DFT and its extensions, such as generalized Kohn-Sham schemes [3], DFT + U [4], and DFT + dynamical mean-field theory [5], its limitations in strongly correlated systems necessitate the development of more accurate many-body approaches

While it is important we continue to further refine and extend DFT-based methods, it is equally important to develop higher-accuracy approaches, such as wave function methods [6] and many-body perturbation theory [7]. DFT struggles when applied to strongly correlated systems such as NiO [8–10]. Recent rapid advances in exascale and GPU computing [6,11] suggest that computationally expensive methods—approaching current practical limits—may become more accessible in the near future. Wave function methods, while highly accurate, are often restricted to the calculation of ground-state properties in smaller systems, requiring significant effort to extract additional information that quite often is not of any use [12].

To address these challenges, many-body perturbation theory (MBPT) approaches, particularly those based on Hedin's formalism [7], provide a promising balance between accuracy and computational efficiency. A real benefit of the approach is that it is *ab initio* and can be extended with the addition of more diagrams describing processes missing from a particular implementation [13]. MBPT also has the benefit that excited state phenomena (required for investigating, e.g., optoelectronic phenomena) are readily computed. Most MBPT implementations are based on the *GW* approximation [14–16] to Hedin's equations. While an improvement over DFT, many implementations are simply first-order perturbations applied to the DFT electronic structure and, as a result, depend on the DFT functional chosen and therefore tend to perform poorly in strongly correlated systems [17,18]. Another key issue with *GW* is the inadvertent cancellation of errors due to missing diagrams, which can lead to seemingly accurate results for specific quantities, such as band gaps, while failing to capture other important physical phenomena and quantities such as the total energy [19,20]. Although this may prove beneficial in certain circumstances, it is important we do not overlook this,

Published by the American Physical Society under the terms of the Creative Commons Attribution 4.0 International license. Further distribution of this work must maintain attribution to the author(s) and the published article's title, journal citation, and DOI.

as certain physical processes may not be captured at all, limiting the method's predictive reliability in unexplored materials. Self-consistent approaches remove the starting-point dependence by iterating the *GW* formalism; however, they can also prove problematic [8,21]. The quasiparticle self-consistent *GW* (QS*GW*) method [9,18,22,23] is one such method that has become popular in recent years. However, conventional QS*GW* ignores vertex effects in both the polarization function and self-energy and, as a result, performs worse in simple systems due to one competing effect now being included and no longer canceling with another missing effect.

To address these shortcomings, researchers have explored incorporating vertex effects in the polarization function and/or self-energy. Inclusion of vertex effects in the polarization function through solving the Bethe-Salpeter equation (BSE) has become popular in recent years [24–26]. Solving the BSE with an effective nonlocal static kernel derived from time-dependent DFT [27–29] has become a common approach. Another approach is to solve the BSE with the kernel $i\delta\Sigma/\delta G$ (the functional derivative of the self-energy with respect to the Green's function) calculated with the *GW* approximation for Σ while neglecting $\delta W/\delta G$ and assuming a static kernel. We used the latter for the QS$G\widetilde{W}$ method in the QUESTAAL code [9,30] to capture excitonic effects in strongly correlated systems such as NiO for optical spectra and to also improve the electronic structure. In those works we calculated W at the level of the random phase approximation (RPA). Although it is an improvement compared with QS*GW*, many effects are still missing from the method, including time-dependent interactions in the BSE and multiexcitonic effects. Time dependence in the interaction kernel was examined in Refs. [31,32] and was shown to strongly affect optical spectra in noble metals [31]. Multiexcitonic effects [33,34] describe the process of a number of interacting electron-hole pairs propagating in the system. These effects are crucial for examining optoelectronic phenomena such as high-harmonic generation [35] and nonlinear effects.

Another effect missing in the QS$G\widetilde{W}$ method is the vertex in the expression for the self-energy, i.e., going beyond the *GW* approximation for Σ. Methods exist for including vertex effects in the self-energy, such as those developed by Kutepov [36,37], showing the significance of these effects in predicting flat, dispersionless bands in materials like the copper halides CuCl and CuBr [9,38]. The multichannel Dyson equation method [39] and the method outlined in Ref. [40] also included vertex effects in the self-energy. Recently, I developed a method for including vertex effects in the self-energy [13], yielding a relatively straightforward expression for the self-energy that extends *GW* by incorporating T-matrix diagrams and second-order statically screened exchange. In that work the benefit of working with the reducible polarization function instead of the irreducible one was made clear. I also examined a similar method with the inclusion of the T-matrix diagrams applied to the case of a positron interacting in finite systems [41], with the additions proving essential for capturing positron physics (describing processes such as virtual positronium formation) and accurately predicting positron binding energies [41] and scattering and annihilation rates [42].

In this work, the beyond-*GW* formalism ($iGW\Gamma$) introduced in Ref. [13], which derives an analytic expression for the interaction kernel $i\delta\Sigma/\delta G$ that appears in the Hedin's equation for the vertex, is extended to examine these same effects in the polarization function $P = -iGG\Gamma$. This approach incorporates time-dependent effects and multiexcitonic interactions, addressing key limitations of conventional BSE formulations. By including the functional derivative of the vertex from $\Sigma = iGW\Gamma$, correlations between separate electron-hole pairs, including higher-order exchange effects, arise. These new additions give rise to effects beyond the standard BSE, including multiexcitonic effects. The derivation is performed in the time domain before being transformed to frequency, and the key steps are presented for the possibility of examining, e.g., time-dependent interactions in the T-matrix and second-order screened exchange diagrams in the future. The method relies on using the reducible polarization function Π instead of the irreducible one, as the screening is simply $v + v\Pi v$, instead of $(1 - vP)^{-1}v$ for the irreducible one. The final expression is depicted with diagrams illustrating the processes included in the formalism. The result is a matrix equation for the reducible polarization function akin to the usual BSE, but now with a frequency-dependent interaction kernel that contains higher-order diagrams. The suppression of self-polarization effects (more pronounced in strongly correlated systems) emerges naturally in this framework. The approach is general, is intuitive, and does not rely on empirical or *ad hoc* parameters or interactions, and when combined with Ref. [13], it is fully self-contained, having the potential to be implemented in various many-body electronic structure and even antimatter [41] software packages.

II. DERIVATION OF THE POLARIZATION FUNCTION

The single-particle Green's function in the frequency domain is

$$G(\boldsymbol{r}, \boldsymbol{r}', \omega) = \sum_n \frac{\varphi_n(\boldsymbol{r})\varphi_n^*(\boldsymbol{r}')}{\omega - \varepsilon_n \pm i\eta}, \tag{1}$$

where φ_n and ϵ_n are the eigenfunctions and eigenvalues of the corresponding Hamiltonian, η is a positive infinitesimal, and the $+$ $(-)$ sign is for particles (holes). n may be a composite index subsuming spin and orbital index or band index and $\boldsymbol{k}$ in extended systems. The inverse Fourier transform $\frac{1}{2\pi}\int G(\boldsymbol{r}, \boldsymbol{r}', \omega)e^{-i\omega t}d\omega$ produces

$$G(\boldsymbol{r}, \boldsymbol{r}', t) = \sum_n \varphi_n(\boldsymbol{r})\varphi_n^*(\boldsymbol{r}')G_n(t), \tag{2}$$

where $G_n(t) = \mp ie^{-i\varepsilon_n t}e^{\mp\eta t}\theta(\pm t)$ and the transformation is calculated using the Cauchy residue theorem

$$\oint_C f(z)dz = \pm 2\pi i \sum \text{residues inside } C, \tag{3}$$

with the contour C taken in the upper plane for $t < 0$ (holes) and in the lower plane for $t > 0$ (particles) to ensure convergence of $e^{\mp\eta t}$ as $|t| \to \infty$. This will be useful for determining the interaction kernel later. The Green's function is diagonal in the basis of the single-particle states $\varphi_n(\boldsymbol{r})$.

The basis of particle-hole states is used throughout this work for quantities involving two particles,

$$S_{\substack{n_1n_2\\n_3n_4}} = \iiiint d\boldsymbol{r}_1 d\boldsymbol{r}_2 d\boldsymbol{r}_3 d\boldsymbol{r}_4 \varphi^*_{n_1}(\boldsymbol{r}_1)\varphi_{n_2}(\boldsymbol{r}_2) \times S(\boldsymbol{r}_1,\boldsymbol{r}_2,\boldsymbol{r}_3,\boldsymbol{r}_4)\varphi_{n_3}(\boldsymbol{r}_3)\varphi^*_{n_4}(\boldsymbol{r}_4), \quad (4)$$

where S is a function of four space coordinates and n index the eigenstates of the single-particle Hamiltonian, denoting a particle (unoccupied ground state) or a hole (occupied ground state). S can also be a two- or three-point function by making use of the Dirac δ function; e.g., the bare Coulomb interaction is $v(\boldsymbol{r}_1,\boldsymbol{r}_2,\boldsymbol{r}_3,\boldsymbol{r}_4) = v(\boldsymbol{r}_1,\boldsymbol{r}_3)\delta(\boldsymbol{r}_1-\boldsymbol{r}_2)\delta(\boldsymbol{r}_3-\boldsymbol{r}_4)$, with $v(\boldsymbol{r}_1,\boldsymbol{r}_3) = 1/|\boldsymbol{r}_1-\boldsymbol{r}_3|$. The transformation back to real space can be performed using the fact that the single-particle states form a complete orthonormal basis. From Hedin's equation for the irreducible polarization function [7,13,43] $P(1,2) = -iG(1,3)G(4,1)\Gamma(3,4;2)$ [with $1 = (\boldsymbol{r}_1,t_1,\sigma_1)$, i.e., space-time and possibly spin and repeated indices on one side of the equality implying summation/integration] the zeroth-order term, i.e., with the vertex approximated as $\Gamma(3,4;2) = \delta(3,4)\delta(4,2)$, in the basis of particle-hole states is[1]

$$P^0_{\substack{n_1n_2\\n_3n_4}}(\omega) = \frac{f_{n_2}-f_{n_1}}{\omega-\varepsilon_{n_1}+\varepsilon_{n_2}+(f_{n_2}-f_{n_1})i\eta}\delta_{n_1,n_3}\delta_{n_2,n_4} \quad (5)$$

with f being the single-particle occupations and 0 (1) indicating a particle (hole), also denoted c (v) for conduction (valence). Note that n_1n_2, denoting a particle-hole pair, will result in a $+i\eta$ shift, i.e., a pair propagating forward in time, and n_1n_2, denoting a hole-particle pair, will result in a $-i\eta$ shift, representing a negative-energy pair propagating backward in time. In the time domain this is

$$P^0_{\substack{n_1n_2\\n_3n_4}}(t) = -ie^{-i(\varepsilon_{n_1}-\varepsilon_{n_2})t}e^{\mp\eta t}\theta(\pm t)\delta_{n_1,n_3}\delta_{n_2,n_4}, \quad (6)$$

where the upper (lower) sign is for n_1,n_2, a particle-hole (hole-particle) pair. This represents the forward propagating noncorrelated electron-hole propagator (or backward traveling hole-particle propagator). Let us now take Hedin's equations for the polarization function and many-body vertex [7,43],

$$\Gamma(1,2;3) = \delta(1,2)\delta(2,3) + \frac{\delta\Sigma(1,2)}{\delta G(4,5)}G(4,6)G(7,5)\Gamma(6,7;2), \quad (7)$$

where Σ is the self-energy and we see the appearance of the functional derivative of the self-energy with respect to the Green's function $\delta\Sigma(1,2)/\delta G(4,5)$, examined in Ref. [13].

As also discussed in Ref. [13], one can work with the reducible polarization function $\Pi = P + Pv\Pi$ instead of the irreducible one P, with

$$\Pi(1,2) = P^0(1,2) + P^0(1;3,4)K(3,4;5,6)\Pi(5,6;2), \quad (8)$$

derived from the three-point definitions of the polarization functions, e.g., $P(1,2;3) = -iG(1,4)G(5,2)\Gamma(4,5;3)$ and $K(3,4;5,6) = v(3,5)\delta(3,4)\delta(5,6) + i\delta\Sigma(3,4)/\delta G(5,6)$.[2] The reducible polarization function is related to the irreducible polarization function via resummation of electron-hole interactions mediated by the bare Coulomb interaction. Here, irreducibility refers to diagrams that cannot be split by cutting a single interaction line. Both Π and P are exact in principle, and either can be used to determine the screened interaction.

The functional derivative of the self-energy is presented in Ref. [13] and, when considered explicitly in the self-energy, $\Sigma(1,2) = iG(1,3)W(4,1)\Gamma(3,2;4)$ (with $W = v + v\Pi v$ being the screened interaction), gives rise to higher-order diagrams that include the second-order screened exchange and diagrams describing the infinite series of two-body ladder interactions between the added particles (or holes as the result of particle removal) and the excited electrons or holes in the system. The expression for the functional derivative of the self-energy in Ref. [13] is derived by also considering the functional derivative of the screening and vertex, which are usually neglected in the BSE. These diagrams will now be included in the expression for the reducible polarization function. To do so, an expression for Π with a time-dependent interaction kernel will need to be derived. If only the first term in Eq. (14) for $i\delta\Sigma/\delta G$ from Ref. [13] is taken (i.e., the GW approximation for Σ is adopted and $\delta W/\delta G$ is ignored) and is also assumed to be static (the $\omega = 0$ contribution), then the usual static BSE [9,24,25,44] can be derived from Eq. (8) (note the kernel will contain a direct v term if we are working with Π that is not present when we are working with P). The screening matrix elements in the basis of particle-hole pairs are then

$$W_{\substack{n_1n_2\\n_3n_4}}(\omega) = v_{\substack{n_1n_2\\n_3n_4}} + \sum_{\substack{n_5n_6\\n_7n_8}} v_{\substack{n_1n_2\\n_5n_6}}\Pi_{\substack{n_5n_6\\n_7n_8}}(\omega)v_{\substack{n_7n_8\\n_3n_4}}, \quad (9)$$

and for the simple vertex $i\delta\Sigma(3,4)/\delta G(5,6) = -W(4,3)\delta(3,5)\delta(4,6)\delta(t_3-t_4)$,

$$\Pi_{\substack{n_1n_2\\n_3n_4}}(\omega) = (f_{n_4}-f_{n_3})\sum_\lambda \frac{X_{n_1n_2,\lambda}X^{-1}_{\lambda,n_3n_4}}{\omega-E_\lambda+i(f_{n_4}-f_{n_3})\eta}, \quad (10)$$

where X and E are the eigenvectors and eigenvalues of the two-particle matrix $H_{\substack{n_1n_2\\n_3n_4}} = (\varepsilon_{n_1}-\varepsilon_{n_2})\delta_{n_1n_3}\delta_{n_2n_4} \pm K_{\substack{n_1n_2\\n_3n_4}}$, with $+$ ($-$) for n_1 a particle (hole), and if H is Hermitian, $X^{-1} = X^\dagger$. In this case, $K_{\substack{n_1n_2\\n_3n_4}} = v_{\substack{n_1n_2\\n_3n_4}} - W_{\substack{n_4n_2\\n_3n_1}}(\omega=0)$. The inclusion of vertex effects means the BSE needs to be solved

[1] Equations for the self-energy and polarization function are often written with an infinitesimal time shift $t = t+\eta$ [e.g., $G(1,2^+)$ to clarify the time ordering at equal times and avoid ambiguities when convolving with instantaneous interactions like the Coulomb interaction]. This notational detail is omitted here, but the standard convention that such shifts are implicitly understood when evaluating expressions involving equal-time singularities is adopted.

[2] The four-point polarization function $P^0(1,2;3,4) = -iG(1,3)G(4,2)$ is defined by "opening the legs" from the definition of the two-point polarization function.

for either P (as in Ref. [9]) or Π. Calculating the BSE for the reducible polarization function has the benefit of enabling the calculation of the poles of W (exactly equal to the poles of Π), and to determine the GW self-energy (i.e., ignoring the vertex in the expression for the self-energy $\Sigma = iGW\Gamma$), we no longer need to construct and invert the dielectric matrix (constructed from the irreducible polarization, calculated from the BSE with K simply equal to $i\delta\Sigma/\delta G$) and perform numerical frequency integration (as in Ref. [18]), nor is, e.g., the plasmon-pole approximation required. Another benefit of calculating Π is that it has the same structure as P^0 above and can be written in the time domain as the sum of a static part and terms describing forward and backward propagation, so the screening matrix is then

$$\boldsymbol{W}(t) = \boldsymbol{v}\delta(t^+) + \boldsymbol{W}^+(t)e^{-\eta t}\theta(t) + \boldsymbol{W}^-(t)e^{+\eta t}\theta(-t), \quad (11)$$

where $t^+ = t + \eta$ and the forward (+) and backward (−) propagating (in time) parts of the correlation contribution to the screening are

$$W^{\pm}_{\substack{n_1n_2\\n_3n_4}}(t) = -i \sum_{\substack{\lambda\\ ph(hp)\\ n_5n_6}} v_{\substack{n_1n_2\\n_5n_6}} X_{n_5n_6,\lambda} X^{-1}_{\lambda,ph(hp)} e^{-iE_\lambda t} v_{\substack{ph(hp)\\n_3n_4}}, \quad (12)$$

with the upper (lower) sign corresponding to $t > (<)\ 0$ and the summation restricted to particle-hole (hole-particle) index pairs, depending on the sign of t. Note that to reduce memory requirements vX can be calculated (or, rather, its two contributions) and transformed into an auxiliary or reduced mixed product basis, as in Refs. [18,45].

To include higher-order terms in the kernel (as in Ref. [13]), a time-dependent interaction kernel is required. This also allows the incorporation of dynamical excitonic effects, as discussed in, e.g., Refs. [31,32]. To do so, let us take Eq. (8) and assume $t_3 = t_5$ and $t_4 = t_6$ and that the kernel is dependent on only a single time difference $t_3 - t_4$, as in Ref. [13], which discusses the diagrams missing from the vertex as a result. The polarization function is also assumed to be time translationally invariant, i.e., dependent on only the time difference $t_1 - t_2$, so one can arbitrarily set $t_2 = 0$, and the polarization function will depend solely on t_1. The Fourier transform is then performed on the expression for the polarization function from the time domain, with the four-point P^0 expressed in terms of the Green's functions. Begin by determining the first-order term in the expansion, $\Pi = P^0 + P^0KP^0 + \cdots$, which can be extended to higher-order terms, while focusing only on the dynamical parts of the interactions for now,

$$\Pi^1_{\substack{n_1n_2\\n_3n_4}}(\omega) = (-i)^2 \iiint dt dt_3 dt_4 e^{i\omega t} G_{n_1}(t_1 - t_3) G_{n_2}(t_4 - t_1) \times K_{\substack{n_1n_2\\n_3n_4}}(t_3 - t_4) G_{n_3}(t_3 - t_2) G_{n_4}(t_2 - t_4), \quad (13)$$

with $t = t_1 - t_2$. n_1n_2 and n_3n_4 are particle-hole or hole-particle index pairs but will be the same when the Tamm-Dancoff approximation (TDA) [46,47] is adopted. To evaluate, use the expression for the Heaviside step function $\theta(t) = \lim_{\eta\to 0^+} 1/2\pi i \int e^{ixt}/(x - i\eta)dx$, and make use of the relation $\int e^{i\omega t}dt = 2\pi\delta(\omega)$ while making sure the contour is placed in the correct plane to ensure the poles are such that terms e^{ixt} do not diverge for complex x as $|t| \to \infty$. The integration over $t = t_1$ (t_2 is set to zero, as discussed above) is carried out initially, producing a δ function that fixes one of the integration variables from the step functions containing t_1, and then the integration variable from the other step function containing t_1 is integrated over using contour integration. The plane chosen to include the poles is dictated by the sign of $t_3 - t_4$. For n_1n_2 and n_3n_4, both particle-hole index pairs,

$$\Pi^1_{\substack{n_1n_2\\n_3n_4}}(\omega) = \frac{i}{\varepsilon_{n_1} - \varepsilon_{n_2} - \omega - i\eta} \int_0^\infty dt_3 \int_0^{t_3} dt_4 \times \left\{ K_{\substack{n_1n_2\\n_3n_4}}(t_3 - t_4) e^{i(\varepsilon_{n_2} - \varepsilon_{n_3} + \omega + i\eta)t_3} e^{i(\varepsilon_{n_4} - \varepsilon_{n_2} - i\eta)t_4} + K_{\substack{n_1n_2\\n_3n_4}}(t_4 - t_3) e^{i(\varepsilon_{n_4} - \varepsilon_{n_1} + \omega + i\eta)t_3} e^{i(\varepsilon_{n_1} - \varepsilon_{n_3} - i\eta)t_4} \right\}, \quad (14)$$

where the terms arise from the two possible time orderings of the interaction. Upon changing the integration variable $t = t_3 - t_4$ we get $\int_0^\infty dt_3 \int_0^{t_3} dt$ for the first term, which can be reordered as $\int_0^\infty dt \int_t^\infty dt_3$, and upon reintroducing the step function we obtain

$$\Pi^1(\omega) = P^0_{\substack{n_1n_2\\n_3n_4}}(\omega) \widetilde{K}_{\substack{n_1n_2\\n_3n_4}}(\omega) P^0_{\substack{n_3n_4\\n_1n_2}}(\omega), \quad (15)$$

where only two indices are shown for P^0 due to the presence of the δ functions in Eq. (5) and

$$\widetilde{K}_{\substack{n_1n_2\\n_3n_4}}(\omega) = \int_0^\infty dt e^{\pm i(\omega + \varepsilon_{n_2} - \varepsilon_{n_3})t} K_{\substack{n_1n_2\\n_3n_4}}(\pm t) + \int_0^\infty dt e^{\pm i(\omega + \varepsilon_{n_4} - \varepsilon_{n_1})t} K_{\substack{n_1n_2\\n_3n_4}}(\mp t), \quad (16)$$

where the upper (lower) sign is for $n_1n_2, n_3n_4 = ph, ph$ (hp, hp). Compared to the work of Marini and Del Sole [31], the kernel has two terms, corresponding to the two time orderings of the interaction, and is expressed as the Laplace transform $[\int_0^\infty e^{-st} f(t)dt]$ calculated at $\mp i(\omega + \varepsilon_{n_2} - \varepsilon_{n_3})$ and $\mp i(\omega + \varepsilon_{n_4} - \varepsilon_{n_1})$, and for direct comparison, we replace n_1n_2, n_3n_4 with v_1c_1, v_2c_2 or c_1v_1, c_2v_2. It is important to note that for the time-reversed part of the interaction (i.e., for a screened interaction that propagates backward in time), the integral is for $t < 0$ (since the backward propagating component is zero for $t > 0$), but this integral is transformed to positive times, which will now require calculating the Laplace transform of $K(-t)$. The kernel can be written as a combination of an instantaneous interaction and a forward and backward propagating interaction, as shown for the screening above, and will be discussed below in relation to the other terms that appear in the expression for the vertex. Focusing only on the screening in the vertex for now (the term that gives rise to the usual BSE, but this time with dynamical effects) produces the kernel [13]

$$K_{\substack{n_1n_2\\n_3n_4}}(t) = v_{\substack{n_1n_2\\n_3n_4}}\delta(t) - v_{\substack{n_4n_2\\n_3n_1}}\delta(t) - \sum_{\substack{n_5n_6\\n_7n_8}} v_{\substack{n_4n_2\\n_5n_6}} \Pi_{\substack{n_5n_6\\n_7n_8}}(-t) v_{\substack{n_7n_8\\n_3n_1}}, \quad (17)$$

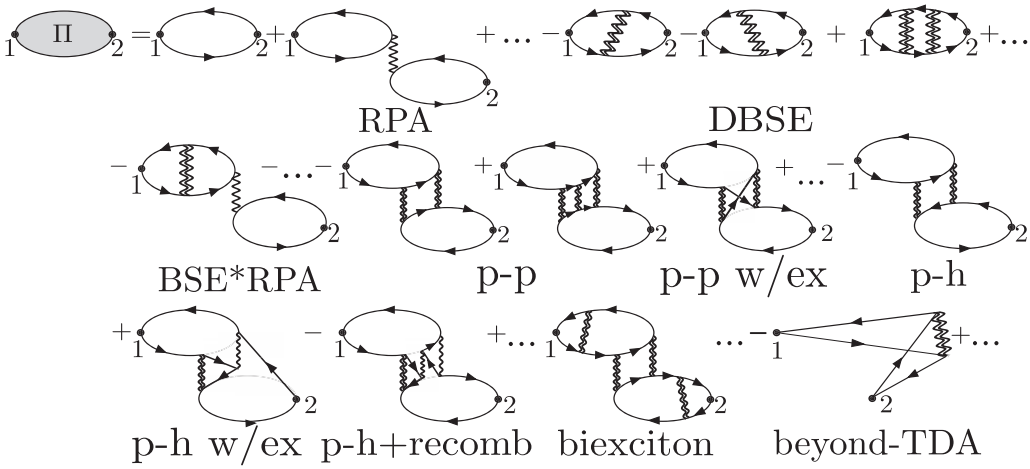


FIG. 1. A subset of the diagrams included in the method for the reducible polarization function. The first two terms are part of an infinite series of bubbles that produce the RPA, followed by the infinite ladder series of time-dependent interactions within these bubbles (the dynamical BSE) that excites further electron-hole pairs. Next is the creation of an electron-hole pair by the excited particle that arises when considering $\delta W/\delta G$ in the interaction kernel (with similar diagrams for the hole) and the infinite series of interactions between the electrons and holes with direct and exchange contributions (from considering $\delta\Gamma/\delta G$ in the interaction kernel). These channels are coupled, as demonstrated by, e.g., BSE*RPA, p-p with exchange, and the multiexcitonic term. The last term is the coupling diagram for the BSE beyond the TDA (see text). In these diagrams, time can be thought to flow horizontally. Straight lines represent propagators (Green's functions), and single (double) wavy lines represent the bare (screened) Coulomb interaction. Suppose the perturbation creating this polarization is the result of adding or removing an electron to or from the system. The contribution to the self-energy from the *GW* channel (i.e., the contributions without vertex effects included in the expression for the self-energy, but included within W) is determined by adding two vertical (instantaneous) Coulomb interaction lines, one that attaches at one end to 1 and another interaction attaching at one end to 2. The other ends of these interactions then connect to the ends of a propagator describing the added electron or hole that generated this polarization.

which in the frequency domain produces the first line from Eq. (24). Note that the time argument in Π appears as $-t$ due to the structure of the equation for the self-energy $\Sigma(1,2) = iG(1,3)W(4,1)\Gamma(3,2;4)$, which simplifies to $G(1,2)W(2,1)$ when the vertex is set to unity. Importantly, this is not necessarily equal to $G(1,2)W(1,2)$, as in Hedin's original work [7]. The screening and polarization are defined slightly differently in that work, as can be seen by comparing the relevant equations in this work (as in Ref. [43]) with (A20) and (A24) in Ref. [7].

Upon including higher-order terms in the expansion of Π, i.e., $\Pi^{(2)} = P^0KP^0KP^0$ we can see that a ladder series of interactions of this form is present in the reducible polarization function $\Pi(\omega) = P^0(\omega) + P^0(\omega)\widetilde{K}(\omega)\Pi(\omega)$. The kernel for n_1n_2 and now n_4n_3 particle-hole (hole-particle) index pairs (i.e., going beyond the TDA and including the coupling between positive- and negative-energy transitions, which is discussed further below), $\widetilde{K}^{\mathrm{C}}$, is

$$\widetilde{K}^{\mathrm{C}}_{\substack{n_1n_2\\n_3n_4}}(\omega) = \int_0^\infty dt e^{\pm i(\varepsilon_{n_3}-\varepsilon_{n_1})t} K_{\substack{n_1n_2\\n_3n_4}}(\mp t) + \int_0^\infty dt e^{\pm i(\varepsilon_{n_2}-\varepsilon_{n_4})t} K_{\substack{n_1n_2\\n_3n_4}}(\pm t), \tag{18}$$

where the upper (lower) sign is for n_1n_2, a particle-hole (hole-particle) pair, and n_3n_4, a hole-particle (particle-hole) pair. Note that this contribution to this representation of the kernel is independent of the frequency ω, which is discussed further below. The coupling between positive- and negative-energy transitions can be understood by considering the BSE in the time domain. Even for an instantaneous interaction kernel, the interaction can occur at a time before or after the external perturbation that polarizes the system (between t_1 and t_2) is present due to an added particle (see Fig. 1). Since the interaction is between positive- and negative-energy propagating pairs (traveling forward and backward in time, respectively) and not restricted to the interval where an external perturbation is present, the interaction is not shifted by the perturbing ω. For time-dependent interactions we can also consider the case of both n_1 and n_2 propagating forward or backward in time. Consider $P^0_{n_1n_2}(1;3,4) = -iG_{n_1}(1,3)G_{n_2}(4,1)$ for $t_3 < t_1$ and $t_4 > t_1$. This involves propagation before or after the external perturbation is present, i.e., when the TDA needs to be relaxed. Therefore, to properly examine these beyond-TDA effects, one would need to extend the particle-hole basis to include particle-particle and hole-hole basis functions. They are used to construct the T-matrix contributions to the self-energy [13] and to include the higher-order vertex effects in the kernel that will now be examined. These beyond-TDA processes describe complex quantum mechanical phenomena such as the emergence of virtual pairs that exist temporarily and describe quantum/vacuum fluctuations (as a result of the uncertainty principle) and/or represent intermediate states mediated by the presence of the time-dependent screening. This is beyond the scope of this work but worth mentioning in the hope of stimulating curiosity.

The functional derivative $i\delta\Sigma/\delta G$ is discussed in detail in Ref. [13], where it is included in the expression for the self-energy, $\Sigma = iGW\Gamma$. This functional derivative and the

resulting vertex from that work will now be used to derive an expression for the kernel in the BSE for the reducible polarization function. In that work, three-body correlated propagation was suppressed (e.g., diagrams that include correlations between the added particle and both the excited electrons and the holes). The diagrams (for the self-energy) that are neglected in that work are presented in Figs. 1 and 2 in Ref. [13], and the corresponding diagrams for the polarization are thus straightforward to deduce. From Eq. (15) in that work, an approximation for the functional derivative is

$$i\frac{\delta\Sigma(3,4)}{\delta G(5,6)} = -W(4,3)\delta(3,5)\delta(4,6) - L_{pp}(3,6;7,8)W(6,3)\chi(7,4;5,8) - L_{ph}(3,5;7,8)W(5,3)\chi(7,4;8,6), \tag{19}$$

where it is assumed that all appearances of W within the functional derivative are instantaneous (which will also be assumed in this work, except for the first term, which is allowed explicit dependence on time to include dynamical excitonic effects) and it is also assumed that the vertices that are attached to W in this recursive series for the vertex (Eq. (14) from Ref. [13]) are approximated as $\Gamma(1,2;3) = \delta(1,2)\delta(2,3)$ and L are two-body correlated propagators that contain correlations between the particles and holes (series of ladder interactions) in the system,

$$\begin{aligned} L_{pp}(1,2;3,4) &= -iG(1,3)G(2,4) + \{-iG(1,5)G(2,6)\}\{-W(6,5)\}L_{pp}(5,6;3,4), \\ L_{ph}(1,2;3,4) &= -iG(1,3)G(4,2) + \{-iG(1,5)G(6,2)\}\{-W(6,5)\}L_{ph}(5,6;3,4), \end{aligned} \tag{20}$$

and

$$\chi(7,4;5,8) = W(4,5)\delta(7,4)\delta(5,8) - W(4,7)\delta(7,5)\delta(4,8), \tag{21}$$

which contain direct and exchangelike contributions, accounting for exchange between electrons and holes from different electron-hole pairs (arising from the first term on the right-hand side of Eq. (19) when considering the recursive series for the vertex).[3] In this work, three-body correlated propagation is suppressed [13]. $L_{ph}(1,2;3,4)$ is the four-point extension of the usual particle-hole propagator, i.e., the irreducible polarization function P. Reference [13] showed that with the inclusion of higher-order vertices, L_{ph} can be replaced by the reducible polarization function Π, which effectively describes recombination with the creation of new electron-hole pairs, as in the RPA. The reducible polarization function is then of the form of the BSE, with kernel

$$\begin{aligned} K(3,4;5,6) = {} & v(3,5)\delta(3,4)\delta(5,6)\delta(t_3-t_5) - W(4,3)\delta(3,5)\delta(4,6) \\ & - L_{pp}(3,6;7,8)W(6,3)\chi(7,4;5,8) - \Pi(3,5;7,8)W(5,3)\widetilde{\chi}^{ph}(7,4;8,6), \end{aligned} \tag{22}$$

where $\widetilde{\chi}^{ph}$ is the interaction in Eq. (21), but with the exchange interaction replaced with a bare interaction (discussed in Fig. 5 and the surrounding text in Ref. [13]).

The particle-particle and hole-hole noncorrelated propagators $L(1,2,3,4) = -iG(1,3)G(2,4)$ for a single time difference are $\mp 1/(\omega - (\varepsilon_{n_1} + \varepsilon_{n_2}) \pm i\eta)$ in frequency or $ie^{-i(\varepsilon_{n_1}+\varepsilon_{n_2})t}e^{\mp\eta t}\theta(\pm t)$ in time, and the kernel is then

$$K_{\substack{n_1n_2\\n_3n_4}}(t) = v_{\substack{n_1n_2\\n_3n_4}}\delta(t) - W_{\substack{n_4n_2\\n_3n_1}}(-t) - \sum_{\substack{n_5n_6\\n_7n_8}} L_{\substack{n_5n_6\\n_7n_8}}(t)\,\tilde{W}_{\substack{n_4n_6\\n_5n_1}}\chi_{\substack{n_7n_2\\n_3n_8}} - \sum_{\substack{n_5n_6\\n_7n_8}} \Pi_{\substack{n_5n_6\\n_7n_8}}(t)\,\tilde{W}_{\substack{n_6n_3\\n_5n_1}}\tilde{\chi}^{ph}_{\substack{n_7n_2\\n_8n_4}}, \tag{23}$$

where $\tilde{W}$ are assumed to be static (see Fig. 1).[4] The reducible polarization function with this kernel is then represented in Fig. 1, and in the frequency domain the kernel is

$$\begin{aligned} \widetilde{K}_{\substack{n_1n_2\\n_3n_4}}(\omega) = {} & v_{\substack{n_1n_2\\n_3n_4}} - v_{\substack{n_4n_2\\n_3n_1}} \mp \sum_{\substack{\lambda,\\ph}}^{n_5n_6} v_{\substack{n_4n_2\\n_5n_6}} X_{n_5n_6,\lambda} \left\{ \frac{X^{-1}_{\lambda,hp(ph)} v_{\substack{hp(ph)\\n_3n_1}}}{\omega + \varepsilon_{n_2} - \varepsilon_{n_3} + E_\lambda \pm i\eta} + \frac{X^{-1}_{\lambda,ph(hp)} v_{\substack{ph(hp)\\n_3n_1}}}{\omega + \varepsilon_{n_4} - \varepsilon_{n_1} - E_\lambda \pm i\eta} \right\} \\ & \mp \sum_{\substack{\alpha,\\n_7n_8}}^{pp'(hh')} \left\{ \tilde{W}_{\substack{n_4p'(h')\\p(h)n_1}} \frac{Y_{pp'(hh'),\alpha} Y^{-1}_{\alpha,n_7n_8}}{\omega + \varepsilon_{n_2} - \varepsilon_{n_3} - \Omega_\alpha \pm i\eta} + \sum_{\substack{\alpha,\\n_7n_8}}^{hh'(pp')} \tilde{W}_{\substack{n_4h'(p')\\h(p)n_1}} \frac{Y_{hh'(pp'),\alpha} Y^{-1}_{\alpha,n_7n_8}}{\omega + \varepsilon_{n_4} - \varepsilon_{n_1} + \Omega_\alpha \pm i\eta} \right\} \chi_{\substack{n_7n_2\\n_3n_8}} \\ & \pm \sum_{\substack{\lambda,\\ph}}^{n_5n_6} \tilde{W}_{\substack{n_6n_3\\n_5n_1}} X_{n_5n_6,\lambda} \left\{ \frac{X^{-1}_{\lambda,ph(hp)} \tilde{\chi}^{ph}_{\substack{p(h)n_2\\h(p)n_4}}}{\omega + \varepsilon_{n_2} - \varepsilon_{n_3} - E_\lambda \pm i\eta} + \frac{X^{-1}_{\lambda,hp(ph)} \tilde{\chi}^{ph}_{\substack{h(p)n_2\\p(h)n_4}}}{\omega + \varepsilon_{n_4} - \varepsilon_{n_1} + E_\lambda \pm i\eta} \right\}, \end{aligned} \tag{24}$$

[3]Reference [13] discusses how $\Gamma(1,2;3) = \delta(1,2)\delta(2,3)$ can be a good approximation with the correct use of noninteracting Green's functions as a result of the Ward identity, which will be discussed further in the conclusions.

[4]The method outlined in this work could be extended to describe time-dependent interactions in the T-matrix diagrams that result from including L in Eq. (19) from Ref. [13].

where the upper (lower) sign is for n_1 a particle, and Y and Ω are the eigenvalues and eigenvectors of the particle-particle (hole-hole) matrix, which in the particle-particle basis is $(\varepsilon_{n_1}+\varepsilon_{n_2})\delta_{n_1n_3}\delta_{n_2n_4} \pm \underset{n_3n_1}{W_{n_2n_4}}$. Note that for convenience the beyond-TDA terms have been omitted. Although this equation appears to be challenging, it is constructed in a way similar to the usual static BSE. The third line is constructed with the same elements as in the first line, and the second line is constructed analogously, instead using the particle-particle (hole-hole) eigenvectors and eigenvalues (requiring the diagonalization of a particle-particle and hole-hole matrix, analogous to the particle-hole matrix) that can also be used to construct the T-matrix contributions to the self-energy in Ref. [13], describing correlations between the added particle (hole) and the excited electrons (holes). As mentioned above, a reduced, mixed-particle basis can be used to reduce the memory and storage demands, and the matrix multiplications can be handled with modern accelerated computing techniques. Once the frequency-dependent kernel is constructed, the usual BSE for the reducible polarization function can be solved by either inversion or diagonalization for the particular frequency. The actual size of the kernel is identical to conventional BSE implementations, such as those in Refs. [24,25,44]; however, the frequency dependence in the kernel now requires the diagonalization (or inversion) of the two-particle matrix for a range of frequencies since the kernel is now frequency dependent. With a frequency-independent interaction kernel the diagonalization to produce the inverse, as in Eq. (10), needs to be performed only once, as opposed to inverting $\omega - H$ a number of times. With a frequency-dependent interaction kernel, however, it will most likely be more efficient to invert the matrix a number of times than to diagonalize it the same number of times. Since the reducible polarization function is such that we know the poles of Π exactly, the convolution between G and Π (to produce the GW + second-order screened exchange self-energy) can be performed analytically, making use of the Cauchy residue theorem, so the screening needs to be calculated only with ω determined from the poles of G and the chosen input energy ω, which is often set equal to the single-particle eigenvalues in many methods, including many QSGW implementations [18,22,23]. Note that the indices are composite indices containing wave vector $\boldsymbol{k}$ in extended systems and their combinations are dictated by the conservation of momentum.

III. CONCLUSIONS

An expression for the kernel in the BSE for the reducible polarization function was derived from Hedin's equations. This includes a number of two-body interactions beyond the usual BSE as a result of the inclusion of the functional derivative of the screening and vertex in $i\delta\Sigma/\delta G$, *ab initio*. These vertex contributions can be included in the kernel after we consider their contribution to the self-energy (giving rise to second-order screened exchange and T-matrix channel contributions [13]). A frequency-dependent interaction kernel incorporating RPA, dynamical excitonic, and multiexcitonic effects (due to correlations between the particles and holes from different electron-hole pairs) was presented. The terms that couple the positive- and negative-energy transitions (i.e., going beyond the Tamm-Dancoff approximation) were also considered and found to be independent of frequency, which is discussed along with an intuitive description of the physical processes described by these terms. In order to present a tractable equation, a number of approximations were made. Three-body correlated propagation was suppressed; the vertices that attached to the screening within the functional derivative $i\delta\Sigma/\delta G$ were approximated as a product of Dirac δ functions (as discussed above), and beyond the first term in $i\delta\Sigma/\delta G$ (the term that appears in the standard BSE), any appearance of W was assumed to be static. In order to construct the kernel, the eigenvectors and eigenvalues of the usual static BSE had to be determined, along with the eigenvectors and eigenvalues of the particle-particle (hole-hole) matrix that produce the T-matrix diagrams in the self-energy [13].

The result is the usual two-body BSE matrix that requires inversion (or diagonalization), but now with a frequency-dependent interaction kernel containing the added diagrams. Since the reducible polarization function is calculated instead of the irreducible one, this matrix needs to be inverted only at a range of known energies (as opposed to requiring the value for a dense range of frequencies required for the numerical frequency convolution to produce the self-energy when we use the irreducible one [18]). The reducible polarization function also has the benefit that macroscopic quantities such as electron energy loss spectroscopy, $1+v\Pi$, and optical absorption spectra, $1/(1+v\Pi)$, are readily computed.

As is the case with the standard BSE, the number of states that can be included will be much lower than the total number of possible states in many systems of interest; however, states not included in the method can still be included at a lower level of theory, e.g., RPA, as discussed in Refs. [9,13]. Self-polarization and correlation effects (significant in strongly correlated systems) will be present in the method; however, they are reduced by the competing direct and exchange interactions and can be mitigated by taking steps to ensure states are not included more than once in the expression for the polarization function and self-energy (another benefit of making use of the reducible polarization function over the irreducible one). The methods can be adopted to consider time-dependent interactions in the T-matrix diagrams and to also include second-order dynamically screened exchange effects. The method is such that crossings of two or more screened interactions are not present. These crossing arise from including $\delta\Gamma/\delta G$; however, the screened interactions that appear in these higher-order terms are assumed to be static. Inclusion of these effects is an avenue for future work. The method is general and can be incorporated into, e.g., the quasiparticle self-consistent GW formalism [9,18], which I previously extended by incorporating excitonic effects with only the static part of W [9].

As discussed extensively in Ref. [13], the use of noninteracting Green's functions in many-body perturbation theory tends to rely on a cancellation with the vertex, dictated by the Ward identity [18,48]. However, since vertices are now being treated explicitly, it may become necessary to abandon the quasiparticle approximation and consider interacting Green's functions (as considered in Ref. [9]) and/or make use of

so-called Z factors (investigated in the examination of time-dependent excitonic effects in Ref. [31]). With the additions discussed above, along with the possibility of including three-body correlation effects [39,49], and the inclusion of spin fluctuations [50] (where T-matrix channels [51] and the particle-particle correlation function that governs superconductivity [52] are calculated) and phonon effects [53], a broadly applicable, high-fidelity *ab initio* approach to solving one-, two-, and even three-particle properties of the many-body problem is within reach. The formalism presented will prove beneficial for researchers studying electronic structure theory, nonlinear optics, and high-harmonic generation in general systems of interest, including strongly correlated materials.

ACKNOWLEDGMENTS

The author would like to thank D. Green (QUB) for fruitful discussions and all those involved in the CCP flagship project: Quasiparticle Self-Consistent *GW* for Next-Generation Electronic Structure, especially M. van Schilfgaarde (NREL, Golden, Colorado) and M. Grüning (QUB).

DATA AVAILABILITY

The data that support the findings of this article are not publicly available. The data are available from the authors upon reasonable request.

[1] P. Hohenberg and W. Kohn, Inhomogeneous electron gas, Phys. Rev. **136**, B864 (1964).
[2] W. Kohn and L. J. Sham, Self-consistent equations including exchange and correlation effects, Phys. Rev. **140**, A1133 (1965).
[3] A. Seidl, A. Görling, P. Vogl, J. A. Majewski, and M. Levy, Generalized Kohn-Sham schemes and the band-gap problem, Phys. Rev. B **53**, 3764 (1996).
[4] V. I. Anisimov, J. Zaanen, and O. K. Andersen, Band theory and Mott insulators: Hubbard U instead of stoner I, Phys. Rev. B **44**, 943 (1991).
[5] A. Kutepov, K. Haule, S. Y. Savrasov, and G. Kotliar, Self-consistent *GW* determination of the interaction strength: Application to the iron arsenide superconductors, Phys. Rev. B **82**, 045105 (2010).
[6] B. S. Fales and B. G. Levine, Nanoscale multireference quantum chemistry: Full configuration interaction on graphical processing units, J. Chem. Theory Comput. **11**, 4708 (2015).
[7] L. Hedin, New method for calculating the one-particle Green's function with application to the electron-gas problem, Phys. Rev. **139**, A796 (1965).
[8] F. Aryasetiawan and O. Gunnarsson, Electronic structure of NiO in the *GW* approximation, Phys. Rev. Lett. **74**, 3221 (1995).
[9] B. Cunningham, M. Grüning, D. Pashov, and M. van Schilfgaarde, QS*GW*: Quasiparticle self-consistent *GW* with ladder diagrams in W, Phys. Rev. B **108**, 165104 (2023).
[10] J. Gebhardt and C. Elsässer, DFT with corrections for an efficient and accurate description of strong electron correlations in NiO, J. Phys.: Condens. Matter **35**, 205901 (2023).
[11] Y.-M. Byun and J. Yoo, GPU acceleration of many-body perturbation theory methods in MOLGW with OpenACC, Int. J. Quantum Chem. **124**, e27345 (2024).
[12] W. Kohn, Nobel lecture: Electronic structure of matter—wave functions and density functionals, Rev. Mod. Phys. **71**, 1253 (1999).
[13] B. Cunningham, Many-body theory beyond *GW*: Towards a complete description of two-body correlated propagation, Phys. Rev. Res. **6**, 043277 (2024).
[14] M. S. Hybertsen and S. G. Louie, Electron correlation in semiconductors and insulators: Band gaps and quasiparticle energies, Phys. Rev. B **34**, 5390 (1986).
[15] F. Aryasetiawan and O. Gunnarsson, The GW method, Rep. Prog. Phys. **61**, 237 (1998).
[16] L. Hedin and S. Lundqvist, *Effects of Electron-Electron and Electron-Phonon Interactions on the One-Electron States of Solids* (Academic Press, New York, 1970), p. 1181.
[17] S. Di Sabatino, J. Koskelo, J. A. Berger, and P. Romaniello, Screened extended Koopmans' theorem: Photoemission at weak and strong correlation, Phys. Rev. B **107**, 035111 (2023).
[18] T. Kotani, M. van Schilfgaarde, and S. V. Faleev, Quasiparticle self-consistent *GW* method: A basis for the independent-particle approximation, Phys. Rev. B **76**, 165106 (2007).
[19] T. Miyake, F. Aryasetiawan, T. Kotani, M van Schilfgaarde, M. Usuda, and K. Terakura, Total energy of solids: An exchange- and random-phase approximation correlation study, Phys. Rev. B **66**, 245103 (2002).
[20] A. El-Sahili, F. Sottile, and L. Reining, Total energy beyond GW: Exact results and guidelines for approximations, J. Chem. Theory Comput. **20**, 1972 (2024).
[21] M. P. Surh, S. G. Louie, and M. L. Cohen, Quasiparticle energies for cubic BN, BP, and BaS, Phys. Rev. B **43**, 9126 (1991).
[22] S. V. Faleev, M. van Schilfgaarde, and T. Kotani, All-electron self-consistent *GW* approximation: Application to Si, MnO, and NiO, Phys. Rev. Lett. **93**, 126406 (2004).
[23] M. van Schilfgaarde, T. Kotani, and S. Faleev, Quasiparticle self-consistent *GW* theory, Phys. Rev. Lett. **96**, 226402 (2006).
[24] F. Sottile, V. Olevano, and L. Reining, Parameter-free calculation of response functions in time-dependent density-functional theory, Phys. Rev. Lett. **91**, 056402 (2003).
[25] A. Marini, R. Del Sole, and A. Rubio, Bound excitons in time-dependent density-functional theory: Optical and energy-loss spectra, Phys. Rev. Lett. **91**, 256402 (2003).
[26] A. Marini, C. Hogan, M. Grüning, and D. Varsano, Yambo: An *ab initio* tool for excited state calculations, Comput. Phys. Commun. **180**, 1392 (2009).
[27] C. Franchini, A. Sanna, M. Marsman, and G. Kresse, Structural, vibrational, and quasiparticle properties of the Peierls semiconductor $BaBiO_3$: A hybrid functional and self-consistent GW + vertex-corrections study, Phys. Rev. B **81**, 085213 (2010).
[28] M. Shishkin, M. Marsman, and G. Kresse, Accurate quasiparticle spectra from self-consistent *GW* calculations with vertex corrections, Phys. Rev. Lett. **99**, 246403 (2007).
[29] F. Bruneval, F. Sottile, V. Olevano, R. Del Sole, and L. Reining, Many-body perturbation theory using the density-functional

concept: Beyond the *GW* approximation, Phys. Rev. Lett. **94**, 186402 (2005).

[30] B. Cunningham, M. Grüning, P. Azarhoosh, D. Pashov, and M. van Schilfgaarde, Effect of ladder diagrams on optical absorption spectra in a quasiparticle self-consistent *GW* framework, Phys. Rev. Mater. **2**, 034603 (2018).

[31] A. Marini and R. Del Sole, Dynamical excitonic effects in metals and semiconductors, Phys. Rev. Lett. **91**, 176402 (2003).

[32] J. R. Williams, N. Tancogne-Dejean, and C. A. Ullrich, Time-resolved exciton wave functions from time-dependent density-functional theory, J. Chem. Theory Comput. **17**, 1795 (2021).

[33] B. H. Ellis, S. Aggarwal, and A. Chakraborty, Development of the multicomponent coupled-cluster theory for investigation of multiexcitonic interactions, J. Chem. Theory Comput. **12**, 188 (2016).

[34] H. S. Lee, M. S. Kim, H. Kim, and Y. H. Lee, Identifying multiexcitons in MoS_2 monolayers at room temperature, Phys. Rev. B **93**, 140409(R) (2016).

[35] V. Chang Lee, L. Yue, M. B. Gaarde, Y.-H. Chan, and D. Y. Qiu, Many-body enhancement of high-harmonic generation in monolayer MoS_2, Nat. Commun. **15**, 6228 (2024).

[36] A. L. Kutepov, Electronic structure of Na, K, Si, and LiF from self-consistent solution of Hedin's equations including vertex corrections, Phys. Rev. B **94**, 155101 (2016).

[37] A. L. Kutepov, Self-consistent solution of Hedin's equations: Semiconductors and insulators, Phys. Rev. B **95**, 195120 (2017).

[38] A. L. Kutepov, Full versus quasiparticle self-consistency in vertex-corrected GW approaches, Phys. Rev. B **105**, 045124 (2022).

[39] G. Riva, P. Romaniello, and J. A. Berger, Multichannel Dyson equation: Coupling many-body Green's functions, Phys. Rev. Lett. **131**, 216401 (2023).

[40] C. Mejuto-Zaera and V. Vlček, Self-consistency in $GW\Gamma$ formalism leading to quasiparticle-quasiparticle couplings, Phys. Rev. B **106**, 165129 (2022).

[41] J. Hofierka, B. Cunningham, C. M. Rawlins, C. H. Patterson, and D. G. Green, Many-body theory of positron binding to polyatomic molecules, Nature (London) **606**, 688 (2022).

[42] C. M. Rawlins, J. Hofierka, B. Cunningham, C. H. Patterson, and D. G. Green, Many-body theory calculations of positron scattering and annihilation in H_2, N_2, and CH_4, Phys. Rev. Lett. **130**, 263001 (2023).

[43] G. Onida, L. Reining, and A. Rubio, Electronic excitations: Density-functional versus many-body Green's-function approaches, Rev. Mod. Phys. **74**, 601 (2002).

[44] E. E. Salpeter and H. A. Bethe, A relativistic equation for bound-state problems, Phys. Rev. **84**, 1232 (1951).

[45] F. Weigend, M. Häser, H. Patzelt, and R. Ahlrichs, RI-MP2: Optimized auxiliary basis sets and demonstration of efficiency, Chem. Phys. Lett. **294**, 143 (1998).

[46] M. Grüning, A. Marini, and X. Gonze, Exciton-plasmon states in nanoscale materials: Breakdown of the Tamm-Dancoff approximation, Nano Lett. **9**, 2820 (2009).

[47] M. Casanova-Páez and L. Goerigk, Assessing the Tamm–Dancoff approximation, singlet–singlet, and singlet–triplet excitations with the latest long-range corrected double-hybrid density functionals, J. Chem. Phys. **153**, 064106 (2020).

[48] R. Kuwahara and K. Ohno, Linearized self-consistent GW approach satisfying the Ward identity, Phys. Rev. A **90**, 032506 (2014).

[49] Y. Pavlyukh, E. Perfetto, and G. Stefanucci, Photoinduced dynamics of organic molecules using nonequilibrium Green's functions with second-born, *GW*, T-matrix, and three-particle correlations, Phys. Rev. B **104**, 035124 (2021).

[50] E. A. Stepanov, V. Harkov, and A. I. Lichtenstein, Consistent partial bosonization of the extended Hubbard model, Phys. Rev. B **100**, 205115 (2019).

[51] D. Nabok, S. Blügel, and C. Friedrich, Electron-magnon scattering in ferromagnets from first principles by combining GW and GT self-energies, npj Comput. Mater. **7**, 178 (2021).

[52] S. Acharya, D. Pashov, F. Jamet, and M. van Schilfgaarde, Controlling T_c through band structure and correlation engineering in collapsed and uncollapsed phases of iron arsenides, Phys. Rev. Lett. **124**, 237001 (2020).

[53] S. Laricchia, C. Eichstaedt, D. Pashov, and M. van Schilfgaarde, Electron-phonon coupling using many-body perturbation theory: Implementation in the questaal electronic structure suite, arXiv:2404.02902.